PAT- a Reliable Path Following Algorithm

Dany Mezher, Bernard Philippe

INSTITUT NATIONAL DE RECHERCHE EN INFORMATIQUE ET EN AUTOMATIQUE

PAT- a Reliable Path Following Algorithm

Dany Mezher, Bernard Philippe

N˚3991

Août 2000

THÈME 4

ISSN 0249-6399 ISRN INRIA/RR--3991--FR+ENG

RENNES

PAT- a Reliable Path Following Algorithm

Dany Mezher*, Bernard Philippe†

Thème 4 — Simulation et optimisation
de systèmes complexes
Projet Aladin

Rapport de recherche n ° 3991 — Août 2000 — 21 pages

Abstract: We present in this paper a new technique for the reliable computation of the $\sigma-$level curve defined by $\Gamma_\sigma(f) = \{z \in \mathbb{C} : |f(z)| = \sigma\}$ where f is a complex function. The proposed algorithm builds an orbit of adjacent equilateral triangles to capture the level curve and uses a bisection algorithm on specific triangle vertices to compute a numerical approximation to $\Gamma_\sigma(f)$. The method provides a guarantee of termination, even in the presence of round-off errors.

Key-words: Path following, pseudo-spectrum, meromorphic functions, orbit, bisection, smallest singular value.

(Résumé : tsvp)

* ESIB-USJ, Campus des Sciences et Technologies, Beirut, Lebanon. Email: dany.mezher@fi.usj.ed.lb.
† IRISA-INRIA, Campus de Beaulieu, 35042 Rennes Cedex, France. Email: bernard.philippe@irisa.fr.

Unité de recherche INRIA Rennes
IRISA, Campus universitaire de Beaulieu, 35042 RENNES Cedex (France)
Téléphone : 02 99 84 71 00 - International : +33 2 99 84 71 00
Télécopie : 02 99 84 71 71 - International : +33 2 99 84 71 71

PAT- un algorithme fiable de suivi de contours

Résumé : Nous présentons dans ce rapport un algorithme fiable de suivi de lignes de niveau définies par $\Gamma_\sigma(f) = \{z \in \mathbb{C} : |f(z)| = \sigma\}$ où f désigne une fonction complexe. L'algorithme proposé commence par construire une suite de triangles équilatéraux le long de $\Gamma_\sigma(f)$ puis utilise un algorithme de dichotomie pour calculer une approximation numérique de $\Gamma_\sigma(f)$. La méthode garantit la terminaison même en arithmétique flottante.

Mots-clé : Suivi de ligne de niveau, pseudo-spectre, fonctions meromorphes, orbite, dichotomie, plus petite valeur singulière

AMS subject classifications. 65H20, 58C07, 65G50, 65H17.

1 Introduction

We present in this paper a path following algorithm to compute the $\sigma-$level curve given by

$$\Gamma_\sigma(f) = \{z \in \mathbb{C} \setminus P : |f(z)| = \sigma\}$$

where f is a complex function defined over $\mathbb{C} \setminus P$ where P is a finite set. The $\sigma-$level curve is a graphic tool that provides the user with information about the sensitivity of the zeros of f. It can be used to localize the set of the approximated zeros obtained by a root finding algorithm in which the stopping criterion is $|f(z)| < \sigma$. It is often used in the case of $f(z) = \sigma_{\min}(A - zI)$, where A is a matrix and $\sigma_{\min}(B)$ is the smallest singular value of B, the $\sigma-$level curve is known as the $\sigma-$pseudo spectrum. It is used to reliably locate the eigenvalues of A [7, 13, 14]. The computation of the smallest singular value is a high cost computation; it can be performed with different algorithms depending on the matrix structure [3, 8, 10, 12].

The most intuitive technique to compute $\Gamma_\sigma(f)$ is to consider a fine grid discretizing the complex plane and to compute $f(z)$ for all grid nodes. This is a highly expensive approach since it requires the evaluation of f at all grid nodes. In order to reduce the computational cost, path following algorithms are used to lower the total number of inspected nodes. Based on continuation with a predictor corrector scheme[1, 7, 5, 11], the process may fail in the case of singular points. In [2], Bekas and Gallopoulos develop the Cobra path following algorithm; a hybrid algorithm that uses a continuation scheme coupled with a fine local grid to compute the pseudo spectrum of a matrix. In [4], Huitfieldt and Ruhe developed a continuation method based on Euler-Newton which predicts singular points along the level curve for large dimensional space. They insert an auxiliary parameter and pass the singular point using an augmented system. We propose a technique based on a bisection process.

The algorithm presented in this paper offers total reliability for the computation of $\Gamma_\sigma(f)$ at a low cost. Furthermore, it provides a guarantee of termination even in the presence of round-off errors. The main idea of the proposed algorithm is to line up a set of equilateral triangles along the level curve and use a bisection algorithm [15] over the triangle vertices to compute $\Gamma_\sigma(f)$. Although this approach only requires the continuity property of f in the domain of interest, we limit our study to the two following cases

1. $f(z) = \sigma_{\min}(A - zI)$ corresponding to the pseudo-spectrum determination,
2. f is a meromorphic function[9] having $\lim_{|z|\to\infty} |f(z)| = +\infty$.

In these cases, $\Gamma_\sigma(f)$ is the union of a finite number of closed curves denoted by $\Gamma_\sigma^{(i)}(f)$ surrounding the zeros of f .

The paper is organized as follows; the mathematical bases are derived in section 2; the algorithm to compute a single component $\Gamma_\sigma^{(i)}(f)$ is presented in section 3, while its complexity is estimated in section 3.1. Section 3.2 provides a backward error analysis and a guarantee of termination. Section 4 reports the technique used to compute all connected components of the level curve. In section 5, numerical tests are described demonstrating the reliability and efficiency of the proposed algorithm.

2 Mathematical bases

We present in this section the mathematical bases of the algorithm used to capture the pattern of a single connected component of the level curve $\Gamma_\sigma^{(i)}(f)$. We start by defining a lattice of uniformly distributed nodes and the corresponding triangular mesh, and then consider a subset $\mathcal{T}_L$ of the mesh triangles which contains the path of $\Gamma_\sigma(f)$; we prove that $\mathcal{T}_L$ is finite set and construct a transformation to generate subsets of $\mathcal{T}_L$ from any given element $T \in \mathcal{T}_L$. The set $\mathcal{T}_L$ will provide the edges from which points of $\Gamma_\sigma(f)$ are computed using a bisection algorithm.

Definition 2.1 *For any $\sigma > 0$, the inside of $\Gamma_\sigma(f)$ is the set*

$$\Delta_\sigma(f) = \{z : |f(z)| < \sigma\}.$$

The closure $\overline{\Delta}_\sigma(f)$ *of* $\Delta_\sigma(f)$ *is bounded and the outside of* $\Gamma_\sigma(f)$ *defined by*

$$\Lambda_\sigma(f) = \{z : |f(z)| > \sigma\}$$

is an unbounded open set.

The fact that $\lim_{|z|\to\infty} |f(z)| = +\infty$ implies that for every $\alpha > 0$, there exists $R_\alpha \in \mathbb{R}^+$ such that $|f(z)| > \alpha$ whenever $|z| > R_\alpha$. The special case of $\alpha = \sigma$ leads to

$$\overline{\Delta}_\sigma(f) \subset \overline{B}(0, R_\sigma)$$

where $\overline{B}(0, R_\sigma)$ is the closed disk with center at 0 and radius R_σ.

Definition 2.2 *Two distinct points* a *and* b *are said to be* σ*-separated if, and only if,*

$$\{a, b\} \cap \overline{\Delta}_\sigma(f) \neq \emptyset \quad \textit{and} \quad \{a, b\} \cap \Lambda_\sigma(f) \neq \emptyset.$$

In this case, the segment $[a, b]$ *is said to be* σ*-separated.*

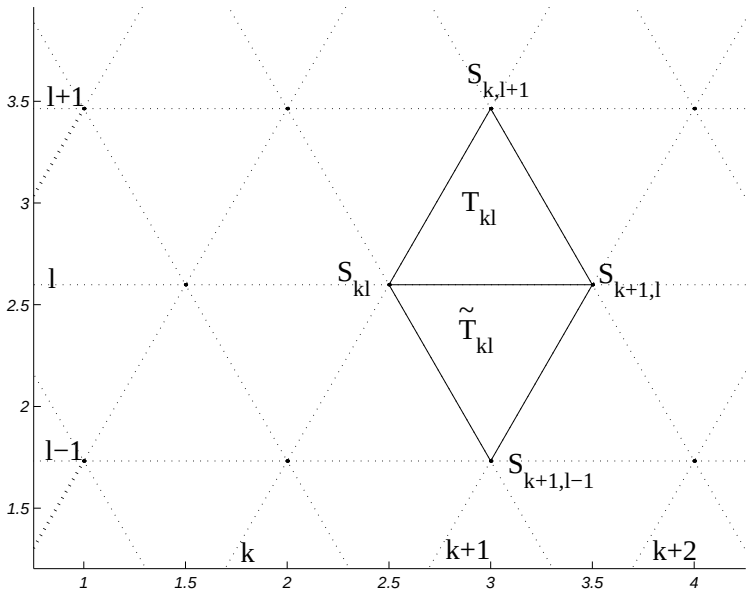

Figure 1: The lattice for $z_i = 0$ and $z_e = 1$

Given $(z_i, z_e) \in \mathbb{C}^2$ *such that* $z_i \neq z_e$*,*

$$S(z_i, z_e) = \{S_{kl} = z_i + k(z_e - z_i) + l(z_e - z_i)e^{i\frac{\pi}{3}}, (k, l) \in \mathbb{Z}^2\}$$

is the uniform lattice (see fig 1) of nodes satisfying

$$|S_{k,l+1} - S_{k,l}| = |S_{k+1,l} - S_{k,l}| = |z_i - z_e|$$

and defining a triangular mesh

$$\Omega(z_i, z_e) = \Psi(z_i, z_e) \cup \tilde{\Psi}(z_i, z_e)$$

where

$$\Psi = \{T_{kl} = \{S_{k,l}, S_{k+1,l}, S_{k,l+1}\} : (k, l) \in \mathbb{Z}^2\}$$

and

$$\tilde{\Psi} = \{\tilde{T}_{kl} = \{S_{k,l}, S_{k+1,l}, S_{k+1,l-1}\} : (k, l) \in \mathbb{Z}^2\}$$

we can easily see that T_{kl} *and* $\tilde{T}_{kl}$ *are equilateral triangles.*

In the following, we denote by $\mathcal{T}_L$ the subset of $\Omega(z_i, z_e)$ where $T \in \mathcal{T}_L$ if, and only if, T has at least two σ-separated vertices.

Proposition 2.1 *For all $z_i \neq z_e$, $\mathcal{T}_L$ is a finite set.*

Proof. For any triangle $T \in \mathcal{T}_L$, there exists a vertex $S_{ij} \in \overline{\Delta}_\sigma(f)$. Since $\overline{\Delta}_\sigma(f)$ is bounded then $S(z_i, z_e) \cap \overline{\Delta}_\sigma(f)$ is a finite set and $card(\mathcal{T}_L) \leq 6 \times card(S(z_i, z_e) \cap \overline{\Delta}_\sigma(f))$. □

We can easily show that if T is an element of $\mathcal{T}_L$ then T has two, and only two, σ-separated edges. Therefore,

Definition 2.3 *The common vertex to the σ-separated sides is called the pivot of T and denoted $p(T)$.*

Definition 2.4 *We define the transformation F (see figure 2)*

$$F(T) = R(p(T), sgn(\sigma - |f(p(T))|) \times \frac{\pi}{3})(T)$$

where

$$sgn(x) = \begin{cases} 1 & \text{if } x \geq 0 \\ -1 & \text{if } x < 0 \end{cases}$$

and $R(z, \theta)$ is the rotation centered at $z \in \mathbb{C}$ with angle θ.

F maps every triangle T of $\mathcal{T}_L$ into a triangle $F(T)$.

Figure 2 shows the four cases of the F transformation, while table (1) presents the corresponding rotation angles.

Transformation Type	T Type	$F(T)$ Type	$p(T)$	$p(F(T))$	θ
II	I	I	$\in \overline{\Delta}_\sigma(f)$	$\in \overline{\Delta}_\sigma(f)$	$\frac{\pi}{3}$
EI	E	I	$\in \Lambda_\sigma(f)$	$\in \overline{\Delta}_\sigma(f)$	$-\frac{\pi}{3}$
EE	E	E	$\in \Lambda_\sigma(f)$	$\in \Lambda_\sigma(f)$	$-\frac{\pi}{3}$
IE	I	E	$\in \overline{\Delta}_\sigma(f)$	$\in \Lambda_\sigma(f)$	$\frac{\pi}{3}$

Table 1: The four possibilities for T and $F(T)$

Proposition 2.2 *For any element $T \in \mathcal{T}_L$, we claim that*

1. *$F(T) \neq T$,*
2. *$p(T)$ is a vertex of $F(T)$,*
3. *T and $F(T)$ are adjacent,*
4. *The common edge to T and $F(T)$ is σ-separated, therefore $F(T) \in \mathcal{T}_L$,*
5. *$p(F(T))$ is a vertex of T,*
6. *$F^2(T) \neq T$,*
7. *if $T \in \Psi(z_i, z_e)$ then $F(T) \in \tilde{\Psi}(z_i, z_e)$ and if $T \in \tilde{\Psi}(z_i, z_e)$ then $F(T) \in \Psi(z_i, z_e)$.*

Proof.

1. Follows from the definition of F.
2. $p(T)$ is the center of the rotation, hence invariant by F.

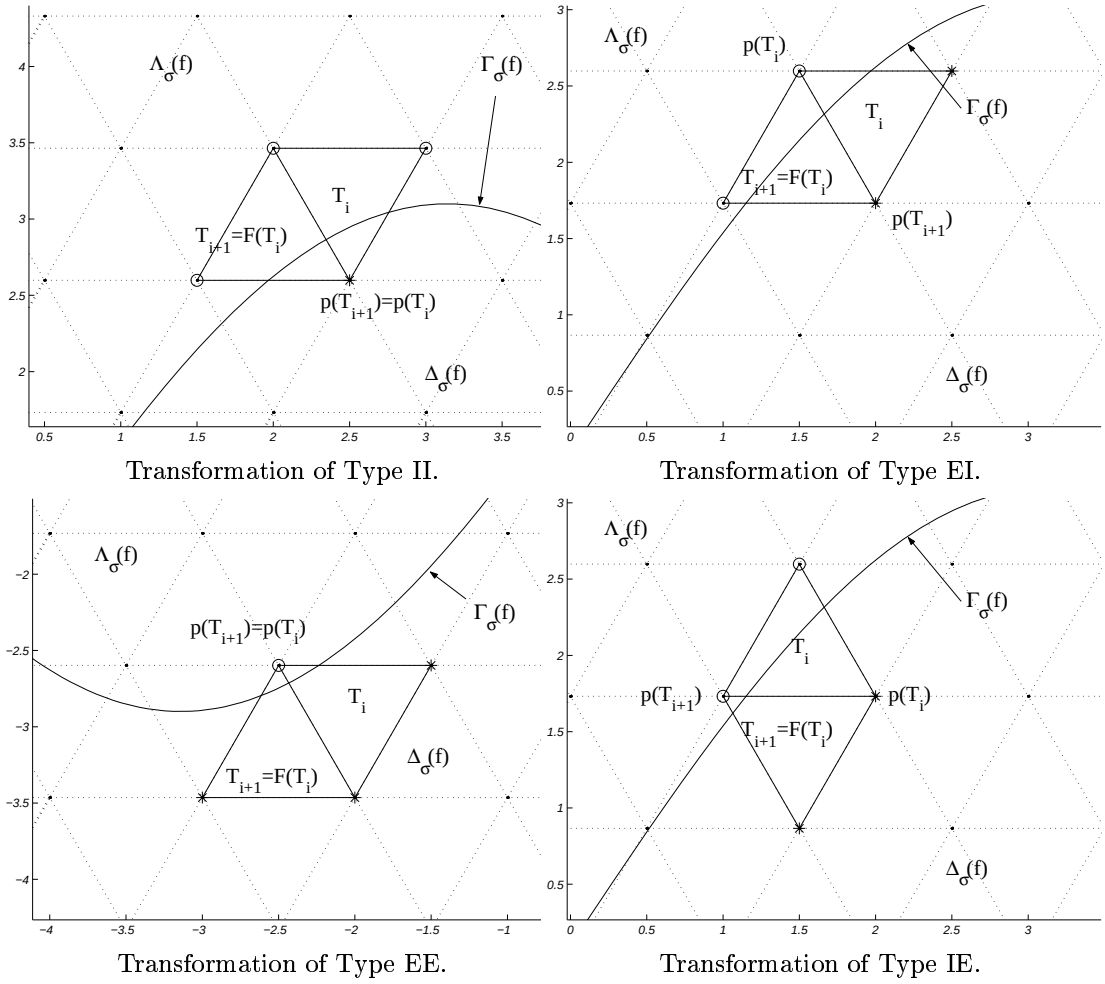

Figure 2: The transformation F

3. Since $F(T)$ is a rotation centered at a vertex of T with angle $\pm\frac{\pi}{3}$, and since T is equilateral T and $F(T)$ are adjacent.

4. $p(T)$ is the common vertex to the $\sigma-$separated sides of T and $p(T) \in F(T)$; the fact that T and $F(T)$ are adjacent leads to the result.

5. Follows from the definition of $p(F(T))$ and 4.

6. We know that T and $F(T)$ are adjacent; furthermore $p(T) \in T \cap F(T)$ and $p(F(T)) \in T \cap F(T)$. Let us consider the two possibilities:

   Either $p(T) = p(F(T)) \rightsquigarrow F^2(T) = R(p(T), \pm\frac{2\pi}{3})(T) \neq T$

   or $p(T) \neq p(F(T))$; in this case

$$\begin{aligned} F^2(T) &= R(p(F(T)), -\theta) \circ R(p(T), \theta)(T) \\ &= \Upsilon[(p(F(T)) - p(T))(1 - e^{-i\theta})](T) \\ &\neq T \end{aligned}$$

   where $\Upsilon[u](x) = x + u$ is the translation of vector u.

7. Immediate.

□

Proposition 2.3 *F is a bijection from $\mathcal{T}_L$ onto $\mathcal{T}_L$.*

Proof. We prove that F is a one-to-one mapping. Let us assume that there exist two triangles T and T' such that

$$F(T) = F(T') \text{ and } T \neq T'.$$

We know from proposition 2.2 that $p(F(T)) \in T$, $p(F(T)) \in F(T)$, $p(F(T)) \in F^2(T)$ and $p(F(T)) \in T'$ therefore

$$p(F(T)) \in T \cap F(T) \cap F^2(T) \cap T'$$

Furthermore, we know that T, $F^2(T)$ and T' are adjacent to $F(T)$. This can only be true if $T' = F^2(T)$; therefore,

$$\begin{aligned} F(T') &= F(F^2(T)) \\ &= F^2(F(T)) \end{aligned}$$

and since $F^2(T) \neq T, \forall T \in \mathcal{T}_L$, then $F(T') \neq F(T)$. This proves that $F : \mathcal{T}_L \to \mathcal{T}_L$ is a one-to-one mapping and therefore a bijection onto the finite set $\mathcal{T}_L$. □

Definition 2.5 *For any given $T \in \mathcal{T}_L$ we define the $F-$orbit of T to be the set $O(T) = \{T_n = F^n(T), n \in \mathbb{Z}\}$.*

Proposition 2.4 *Let $O(T)$ be the $F-$orbit for a given triangle T;*

1. *$O(T)$ is a finite set.*
2. *If $n = card(O(T))$ then n is even and is the smallest positive integer such that $T_n = T$.*
3. *$\sum_{i=0}^{n-1} \theta_i = 0 \quad (2\pi)$ where θ_i is the rotation angle of F for triangle T_i.*
4. *If $O(T')$ is the $F-$orbit for a triangle T' then $O(T) = O(T')$ or $O(T) \cap O(T') = \emptyset$.*

Proof.

1. $O(T) \subset \mathcal{T}_L$ and $\mathcal{T}_L$ is a finite set.

2. Since $T_n \in O(T)$, there exists an integer j such that, $0 \leq j < n$ and $T_n = T_j$. Therefore,

$$T_{n-1} = T_{j-1}$$

This is only true if $j = 0$, otherwise $card(O(T)) < n$.

The fact that n is even follows because T and $F(T)$ belong to two disjoint sets $\Psi(z_i, z_e)$ and $\tilde{\Psi}(z_i, z_e)$.

3. Let $O(T_0) = \{T_0, T_1, ..., T_{n-1}\}$ be the $F-$orbit of T_0; in the following, $\{P_i, S_i, U_i\}$ denotes the triangle T_i such that P_i is the pivot of T_i and $(\overrightarrow{P_iS_i}, \overrightarrow{P_iU_i}) = \theta_i \ \ (2\pi)$ such that $F(T_i) = R(P_i, \theta_i)(T_i)$. Therefore, we can say

$$T_i \cap T_{i+1} = [P_i, U_i] = [P_{i+1}, S_{i+1}]$$

We have now two cases; either T_i and T_{i+1} are of the same type (I or E, see Table 1) and therefore $P_{i+1} = P_i$ and $S_{i+1} = U_i$ leading to

$$\overrightarrow{P_{i+1}S_{i+1}} = \overrightarrow{P_iU_i}$$

or T_i and T_{i+1} are of different type, and therefore $P_{i+1} = U_i$ and $S_{i+1} = P_i$ and

$$\overrightarrow{P_{i+1}S_{i+1}} = -\overrightarrow{P_iU_i} \tag{1}$$

Let us consider the sum

$$\begin{aligned} \sum_{i=0}^{n-1} \theta_i &= \sum_{i=0}^{n-1} (\overrightarrow{P_iS_i}, \overrightarrow{P_iU_i}) \ \ (2\pi) \\ &= (\overrightarrow{P_0S_0}, \overrightarrow{P_0S_0}) + k\pi \ \ (2\pi) \end{aligned}$$

where k is the number of triangles satisfying (1). Since $F_n(T_0) = T_0$, we can claim that k is even; finally

$$\sum_{i=0}^{n-1} \theta_i = 0 \ \ (2\pi)$$

4. Let T" be an element of $O(T) \cap O(T')$; there exists two integers i, j such that

$$T" = F_i(T) = F_j(T') = F_{n+j}(T') \Rightarrow T = F_{j+n-i}(T')$$

where $n = card(O(T'))$, leading to $O(T) \subset O(T')$. In the same way we can prove that $O(T') \subset O(T)$.

□

3 The path following algorithm

In this section, we analyze the implementation of the path following algorithm presented in figure 3. The goal of this algorithm is twofold:

1. Find a suitable lattice and the corresponding $F-$orbit O to capture the pattern of a connected component of the level curve. We start by determining two points $z_i \in \overline{\Delta}_\sigma(f)$ and $z_e \in \Lambda_\sigma(f)$ such that $|z_i - z_e| = \tau$ where τ defines the resolution of the lattice. The two points z_i and z_e are used to generate the lattice $S(z_i, z_e)$ where $T_0 = \{S_{00}, S_{10}, S_{01}\}$ is an element of $\mathcal{T}_L$ which generates the $F-$orbit.

   In our implementation, the technique used to compute z_i and z_e is :

(a) Startup

Given σ,τ and $\tilde{z}_0$ such that $|f(\tilde{z}_0)| \leq \sigma$
for k=1,2,...
    $\tilde{z}_k = \tilde{z}_0 + 2^{k-1}\tau e^{i\theta}$
    if $|f(\tilde{z}_k)| > \sigma$ **break**
end for
Use a bisection algorithm over $\tilde{z}_0$ and $\tilde{z}_k$,
    to compute z_i and z_e where
    $|f(z_i)| \leq \sigma < |f(z_e)|$ and $|z_i - z_e| = \tau$
Let $T_0 = \{z_i, z_e, z_i + (z_e - z_i)e^{\frac{i\pi}{3}}\} \in \mathcal{T}_L$ be an initial triangle

(b) building the $F-$orbit of T_0

for $i = 0, 1, 2, ...$
    $T_{i+1} = F(T_i)$
    if $T_{i+1} = T_0$ **break**
end for

Figure 3: Path Following algorithm

- Given $\tilde{z}_0$ such that $|f(\tilde{z}_0)| \leq \sigma$, consider the complex sequence defined by

$$\tilde{z}_{k+1} = \tilde{z}_0 + 2^k \tau e^{i\theta}$$

  where θ is a random angle; in this case,

$$\lim_{k \to +\infty} |f(\tilde{z}_k)| = +\infty.$$

  Let $k_0 \in \mathbb{N}^*$ be a value of k such that $|f(\tilde{z}_{k_0})| > \sigma$
- use a bisection algorithm, starting from $\tilde{z}_0$ and $\tilde{z}_{k_0}$, to compute the two points z_i and z_e.

The $F-$orbit is built by successively applying F from the initial triangle T_0.

2. Find an approximation to $\Gamma_\sigma^{(i)}(f)$; this is achieved by performing, over each element of O, a bisection algorithm starting from the σ-separated vertices. The choice of the bisection algorithm, presented in figure 4, is due to its reliability.

3.1 Complexity

Let $O(T)$ be the $F-$orbit of T built to compute a numerical approximation of a connected component of a level curve $\Gamma_\sigma(f)$; we limit our study to the case[1] where $card(O(T)) > 6$.

Proposition 3.1 *The number n of triangles needed to capture the pattern of a level curve of length l satisfies*

$$\frac{l}{\tau} \leq n \leq \frac{10l}{\tau\sqrt{3}}.$$

[1] It is obvious that the smallest orbit has 6 elements.

Let x, y be two complex values such that $|f(x)| \leq \sigma$ and $|f(y)| > \sigma$
while $|x - y| > \rho|x|$
  $m = \frac{x+y}{2}$
  if $|f(m)| > \sigma$ **then**
    $y = m$
  else
    $x = m$
  end if
end while

Figure 4: The bisection algorithm

Proof. For any given element $U \in O(T)$, there exists an integer $0 \leq k < 5$ such that $p(F^k(U)) \neq p(F^{k+1}(U))$, otherwise $F^6(U) = U$ and $card(O(T)) = 6$.

In the following, we denote by $V = F^k(U)$, $W = F(V)$ and $[x, y] = V \cap W$. We may assume that $x = p(V)$ and $y = p(W)$. Let v be the third vertex of V and w the third vertex of W; the two segments $[x, v]$ and $[y, w]$ are σ-separated and parallel. If $z^{(v)} \in [x, v] \cap \tilde{\Gamma}_\sigma(f)$ and $z^{(w)} \in [y, w] \cap \tilde{\Gamma}_\sigma(f)$ then

$$|z^{(v)} - z^{(w)}| \geq d([x, u], [y, v]) = \frac{\tau\sqrt{3}}{2}.$$

Therefore, we are guaranteed to progress by a distance not smaller than $\frac{\tau\sqrt{3}}{2}$ for five consecutive triangles. □

3.2 Round-off errors and termination

As shown in proposition 2.4, the process terminates when $F(T_k) = T_0$. To guarantee the process termination even in the presence of round-off errors, we use integer coordinates to identify the lattice nodes. Therefore, the node S_{kl} is identified by the two integers k and l and the evaluation of $f(S_{kl})$ requires the evaluation of

$$f(z_i + k(z_e - z_i) + l(z_e - z_i)e^{\frac{i\pi}{3}}).$$

3.2.1 Backward error analysis

Let us now consider the effect of roundoff errors on the evaluation of $f(S_{kl})$ where S_{kl} is a mesh node. It might be possible that in some cases the computed value $fl(|f(S_{kl})|)$ and the exact value $|f(S_{kl})|$ enclose the $\sigma-$level curve and therefore, the constructed orbit differs from the exact one. We shall prove that the computed orbit is the exact orbit of a function g approximating f within a precision defined by the floating point arithmetic precision.

In the following, we define the *forward error* e_{kl} of the evaluation of $f(S_{kl})$ by

$$fl(f(S_{kl})) = f(S_{kl}) + e_{kl}$$

furthermore, we assume that the evaluation of f is performed by a reliable and stable computation which means that:

$$|e_{kl}| = O(\epsilon\eta_{kl})$$

where ϵ is the machine precision parameter and $\eta_{S_{kl}} = \max(\epsilon, |f(S_{kl})|)$; this implies that

$$\max_{z \in S(z_i, z_e)} \frac{|e_z|}{\eta_z} = O(\epsilon)$$

Theorem 3.1 *For any given $\sigma-$level curve and any given acceptable*[2] *T, we consider the numerically computed $F-$orbit $\tilde{O}(T)$ computed using a floating point arithmetic precision parameter ϵ. The $F-$orbit $\tilde{O}(T)$ may be considered as the exact $F-$orbit for a function g satisfying*

$$||\frac{f-g}{\eta}||_\infty = O(\epsilon)$$

where

$$\eta(z) = \begin{cases} \eta_z \text{ if } z \text{ is a mesh node,} \\ \max(\eta_u, \eta_v) \text{ if } z \in]u,v[\text{ edge of the lattice,} \\ \max(\eta_u, \eta_v, \eta_w) \text{ if } z \text{ belongs to a triangle } \{u,v,w\} \text{ of the mesh.} \end{cases}$$

Proof. Since the forward error is defined at each vertex of the mesh, we can linearly interpolate it on each mesh triangle based on the values at the vertices: for any z belonging to the triangle $\{u,v,w\}$, we consider (α,β,γ) the barycentric coordinates of z where $\alpha \geq 0$, $\beta \geq 0$, $\gamma \geq 0$ and $\alpha+\beta+\gamma = 1$; in this case, $z = \alpha u + \beta v + \gamma w$. By definition, $e(z) = \alpha e_u + \beta e_v + \gamma e_w$. The function g defined by $g(z) = f(z) + e(z)$ interpolates the computed evaluations of f over the mesh and

$$\begin{aligned} \frac{|e(z)|}{\eta(z)} &\leq \alpha\frac{|e_u|}{\eta(z)} + \beta\frac{|e_v|}{\eta(z)} + \gamma\frac{|e_w|}{\eta(z)} \\ &\leq \alpha\frac{|e_u|}{\eta_u} + \beta\frac{|e_v|}{\eta_v} + \gamma\frac{|e_w|}{\eta_w} \\ &\leq O(\epsilon) \end{aligned}$$

□

When the orbit $O(T)$ is built, the bisection process is run to obtain a polygon with vertices $\{z^{(i)}\}_{i=0,n-1}$ such that $|z^{(i+1)} - z^{(i)}| \leq \tau$. In the stopping criterion $|x-y| \leq \rho|x|$, ρ is chosen an order of magnitude larger than ϵ and smaller than τ

$$\epsilon \ll \rho \leq \tau.$$

4 Computing disjoint connected components of $\Gamma_\sigma(f)$

Given a set $\mathcal{I}$ of points of $\overline{\Delta}_\sigma(f)$, and eventually another set of points $\mathcal{E}$ of $\Lambda_\sigma(f)$, we develop in this section a technique to compute all connected components surrounding the points of $\mathcal{I}$. In practice, $\mathcal{I}$ and $\mathcal{E}$ might be the sets of zeros and poles of f obtained by a root finding algorithm.

Suppose that the procedure described in figure 3 has been performed and a component $\Gamma_\sigma^{(0)}(f)$ of the level curve computed. Let z_i and z_e be the two points which generate the lattice $S(z_i, z_e)$. We present the procedure used to localize the missing components.

The $\sigma-$level curve has a missing component when there exists $z \in \mathcal{I}$ not surrounded by $\Gamma_\sigma^{(0)}(f)$. To identify if $z \in \mathcal{I}$ is not surrounded, we consider the criterion

$$Ind_{\Gamma_\sigma^{(0)}(f)}(z) = 0$$

where

$$Ind_{\tilde{\Gamma}_\sigma(f)}(z_e) = \frac{1}{2i\pi}\int_{\tilde{\Gamma}_\sigma(f)} \frac{dz}{z-z_e}$$

We know that [9] $Ind_{\tilde{\Gamma}_\sigma(f)}(z_e)$ is an integer-valued function which is 0 if, and only if, z_e is not surrounded by the level curve $\tilde{\Gamma}_\sigma(f)$. Numerically, $Ind_{\tilde{\Gamma}_\sigma(f)}(z_e)$ can be evaluated by the sum

$$Ind_{\tilde{\Gamma}_\sigma(f)}(z_e) = \frac{1}{2\pi} \sum_{z^{(i)} \in \tilde{\Gamma}_\sigma(f)} \arg\frac{z^{(i+1)} - z_e}{z^{(i)} - z_e} \tag{2}$$

[2] An acceptable triangle is triangle having $fl(Sgn(|f(z)| - \epsilon)) = Sgn(|f(z)| - \epsilon)$ for the three vertices.

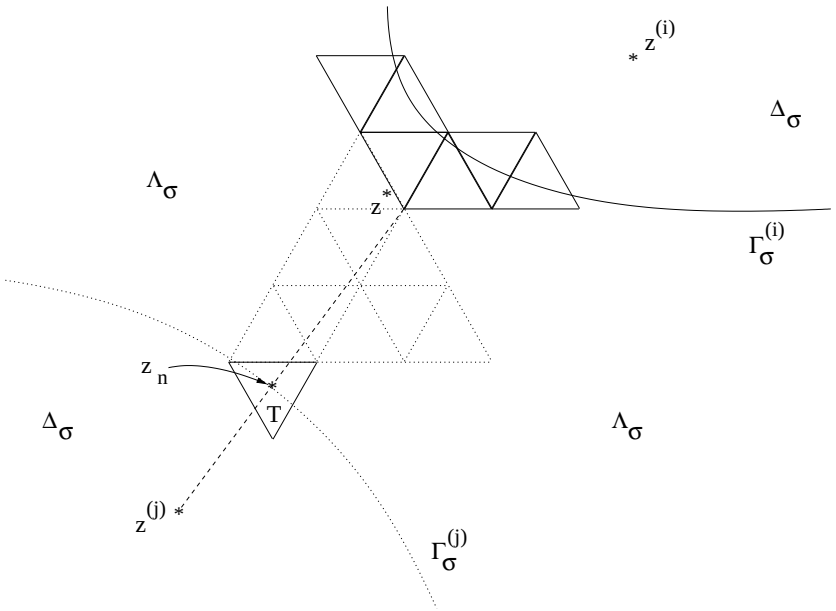

Figure 5: Capturing multiple components of the level curve

where $z^{(i)}$ and $z^{(i+1)}$ are two consecutive points of $\Gamma_\sigma^{(i)}(f)$.

To locate the component surrounding $z \in \mathcal{I}$, we choose $z^* \in \Lambda_\sigma(f)$ where z^* is the closest vertex to z of the triangles in the computed $F-$orbits (see fig 5). A bisection algorithm over z and z^* is used to locate a point $z^{(k)} = [z, z^*] \cap \Gamma_\sigma(f)$ and the triangle $T \in \Omega(z_i, z_e)$ having $z^{(k)}$ as an internal point. This choice is of interest because the orbits of different components are not connected and the triangle $T \notin \cup_j \Gamma_\sigma^{(j)}(f)$ for all already computed components; therefore, the $F-$orbit of T will capture a new component of the level curve. We repeat the above procedure until all points in $\mathcal{I}$ get surrounded by $\cup_j \Gamma_\sigma^{(j)}(f)$.

For any point $z^* \in \mathcal{E}$, we consider the closest vertex z of the computed $F-$orbits to z^*. If $z \in \overline{\Delta}_\sigma(f)$, we can build a new component separating z from z^* by using the previous procedure. This is specially useful when the poles of the function f create holes in $\overline{\Delta}_\sigma(f)$ (see Figure 10).

In the case of close components, the path following algorithm might *jump* from one component to another; therefore, it might capture the pattern of multiple components of the level curve as if they were one. Figures 7, shows different behaviors of the algorithm for the same level curve $\sigma = 0.28$ of the function defined in (4). In (4), A is normal; therefore, the level curve is composed of the set of circles centered at the eigenvalues $z_k = e^{\frac{2ik\pi}{11}}$ with radius $r = 0.28$. In figure 7-(a), the algorithm jumps from one circle to another whereas, in figure 7-b, the algorithm keeps track of the two circles; this is mainly due to the relative orientation of the triangles with respect to the level curve.

5 Test problems and numerical results

In this section, we report some numerical results obtained by using a Matlab prototype implementation[3] of the procedure previously described to demonstrate its performance. Table 2 gathers the statistics concerning the different numerical examples whereas Figure 15 presents the ratio

$$\frac{\text{Effective Number of triangles}}{\text{Maximum number of triangles}}$$

The first test function is the polynomial

$$f(z) = z^{11} - 1 \tag{3}$$

[3]This code is available via anonymous ftp from the site `ftp.irisa.fr/local/aladin/philippe/PAT` .

Given σ,τ and $Z = \{z^{(i)} : f(z^{(i)}) = 0\}$
Select any $z^{(0)} \in Z$
Use algorithm 3 to compute a component $\Gamma_\sigma^{(0)}(f)$
  and the corresponding $F-$orbit $O(T_0)$;
  let z_i and z_e be the complex values used
  to generate the lattice.
Set $O = O(T_0)$
Set $Z_e = \{z^{(i)} : z^{(i)} \in Z, Ind_{\Gamma_\sigma^{(0)}(f)}(z^{(i)}) \neq 0\}$
Set $Z = Z - Z_e$
while $Z \neq \emptyset$
    Select $z^{(i)} \in Z$
    Find the complex z^* that minimizes $|z^* - z^{(i)}|$ where z^*
      is a vertex of a triangle in O and $z^* \in \Lambda_\sigma(f)$
    Use a bisection algorithm to compute $z = [z^{(i)}, z^*] \cap \Gamma_\sigma(f)$
    Let T_1 be the triangle of the lattice $S(z_i, z_e)$ built in
      algorithm 3 having z as an internal point
    Compute a new component $\Gamma_\sigma^{(1)}(f)$, and the corresponding
      $F-$orbit $O(T_1)$ using algorithm 3 starting from step (b)
    $Z_e = \{z^{(i)} : z^{(i)} \in Z, Ind_{\Gamma_\sigma^{(1)}(f)}(z^{(i)}) \neq 0\}$
    $O = O \cup O(T_1)$
    $Z = Z - Z_e$
end while

Figure 6: Computing disjoint components of $\Gamma_\sigma(f)$

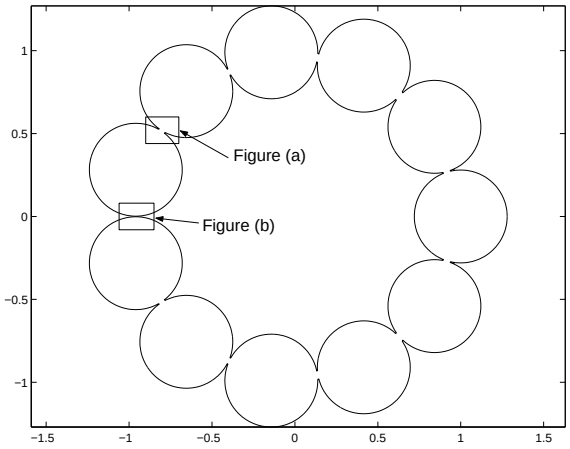

$\tilde{\Gamma}_\sigma(f)$ for $f(z) = \sigma_{\min}(A - zI)$ with $\sigma = 0.28$ and $\tau = 0.01$.

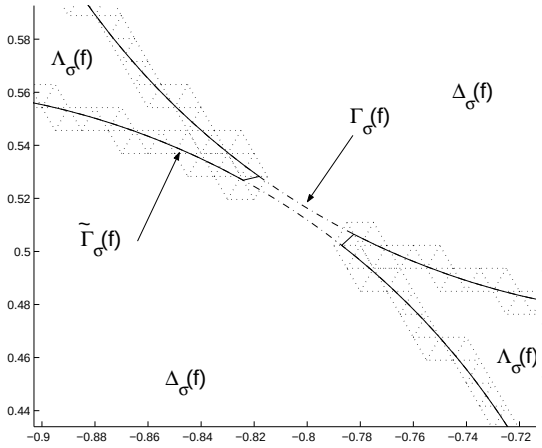

Fig. (a) - The path following algorithm jumps from one circle to another.

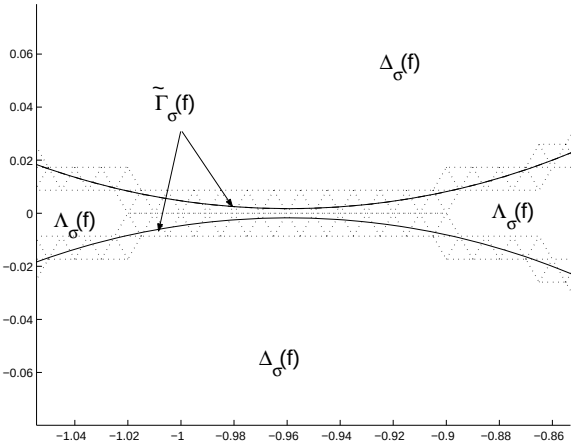

Fig. (b) - The algorithm keeps track of two distinct circles.

Figure 7: Merging two close components of the level curve $\Gamma_\sigma(f)$ for $\sigma = 0.28, \tau = 0.01$ and $f(z) = \sigma_{\min}(A - zI)$.

where $f(z)$ has eleven zeros $z_k = e^{\frac{i2k\pi}{11}}$. We have run the code for $\mathcal{I} = \{z_k\}$, $\mathcal{E} = \{\}$, $\sigma = 1$, 1.005, 1.05, 1.2, 0.999, 0.9, 0.8 and $\tau = 0.01$. In figures 8 and 9 we plot the corresponding level curves.

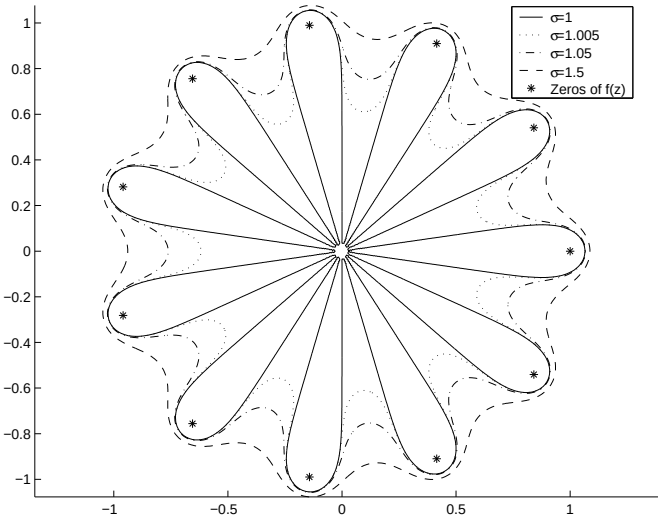

Figure 8: Level curves for $f(z) = z^{11} - 1$ with $\tau = 0.01$

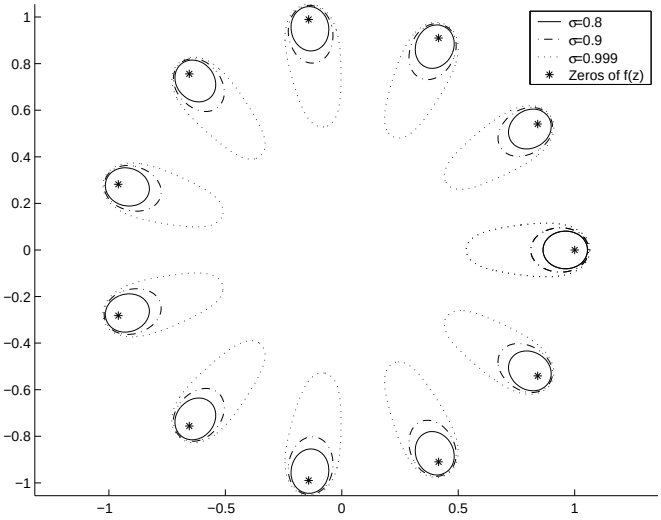

Figure 9: Level curves for $f(z) = z^{11} - 1$ and $\tau = 0.01$

The second test function is given by

$$f(z) = \frac{z^5 - 1}{z}$$

This function has 5 zeros on the unitary circle and a pole at the origin. We present in figures 10 and 11 the level curves for $\mathcal{I}$ being the set of zeros of f, $\mathcal{E} = \{0\}$, $\sigma = 1.65$, 2, 3 and $\tau = 0.01$, 0.1. Note that in this case, the use of the $\mathcal{E}$ enables us to determine the hole in $\overline{\Delta}_\sigma(f)$ centered at 0.

Finally, we consider the two pseudo-spectrum problems defined by

$$f(z) = \sigma_{\min}(A - zI)$$

where σ_{min} is the smallest singular value. In the first case, we consider the orthogonal matrix

$$A = \begin{pmatrix} 0 & 1 \\ I_{10} & 0 \end{pmatrix} \tag{4}$$

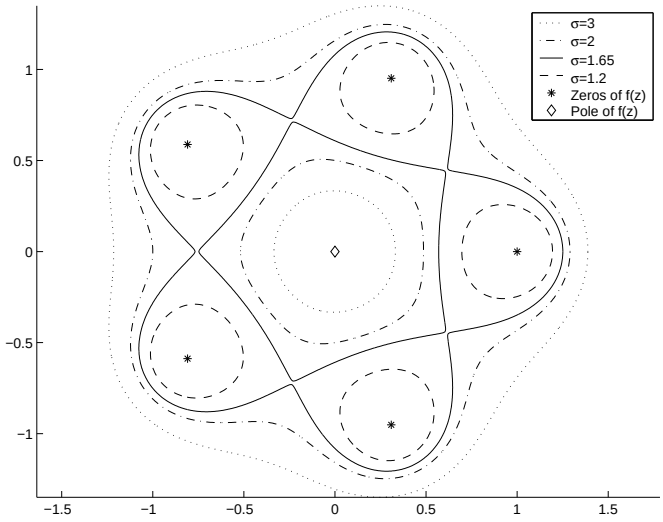

Figure 10: Level curves for $f(z) = \frac{z^5-1}{z}$ with $\tau = 0.01$

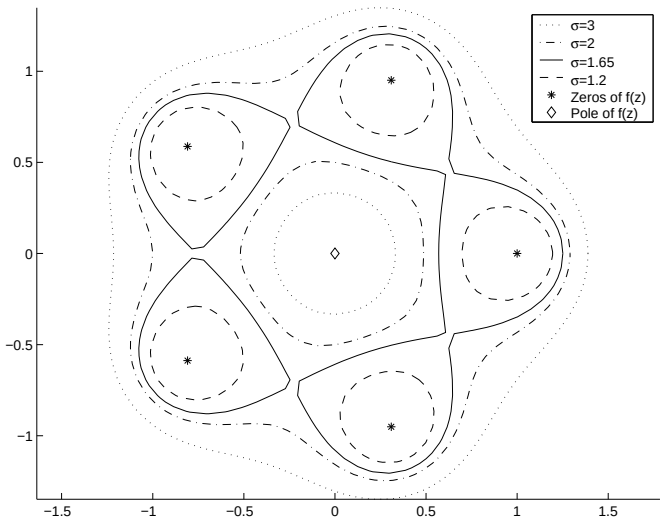

Figure 11: Level curves for $f(z) = \frac{z^5-1}{z}$ with $\tau = 0.1$

and I_{10} is the 10×10 identity matrix. The matrix presented in 4 is normal, therefore, the level curve for a given σ is the union of the circles centered at the eigenvalues with radius σ. Figures 12 and 13 show the level curves for $\sigma = 0.28, 0.3, 0.5, 1$ and $\tau = 0.01, 0.1$. For the particular case where $\sigma = 0.28$, adjacent circles are only separated by a distance $d \simeq 0.0034 < \tau$; therefore, the path following algorithm jumps from one component of the level curve to another. Next, we consider the non normal `GRCAR` matrix $A \in \mathbb{R}^{100\times 100}$ given by

$$A = \begin{pmatrix} 1 & 1 & 1 & 1 & 0 & \dots & \dots & 0 \\ -1 & 1 & 1 & 1 & 1 & 0 & \dots & 0 \\ 0 & \ddots & \ddots & \ddots & \ddots & \ddots & \ddots & \vdots \\ \vdots & \ddots & \ddots & \ddots & \ddots & \ddots & \ddots & 0 \\ \vdots & & \ddots & \ddots & \ddots & \ddots & \ddots & 1 \\ \vdots & & & \ddots & \ddots & \ddots & \ddots & 1 \\ \vdots & & & & \ddots & \ddots & \ddots & 1 \\ 0 & \dots & \dots & \dots & \dots & 0 & -1 & 1 \end{pmatrix} \tag{5}$$

This matrix is ill-conditioned with respect to its eigensystem. Figure 14 shows the level curves for the input presented in the following

σ	τ	$\mathcal{I}$	$\mathcal{E}$
8.730×10^{-12}	0.01	$\{2i, -2i\}$	$\{\}$
4.585×10^{-5}	0.01	$\{1.25\}$	$\{\}$
4.712×10^{-3}	0.01	$\{-0.5 - 2i\}$	$\{\}$
1.494×10^{-1}	0.01	$\{-0.75 - 2i\}$	$\{\}$

Since the evaluation of f is more expensive than the previous tests, we used a parallel implementation of the code [6]. This example shows that the proposed algorithm copes easily with directional discontinuities along the level curve.

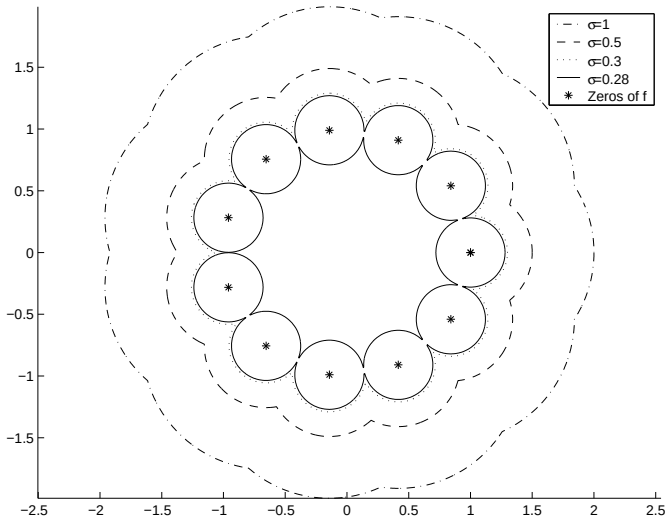

Figure 12: Level curves for $f(z) = \sigma_{\min}(A - zI)$ with $\tau = 0.01$

6 Conclusion

We have shown that the combination of the $F-$orbit with a bisection algorithm results in a numerically stable path following strategy. Construction of the $F-$orbit is guaranteed to terminate even in the presence

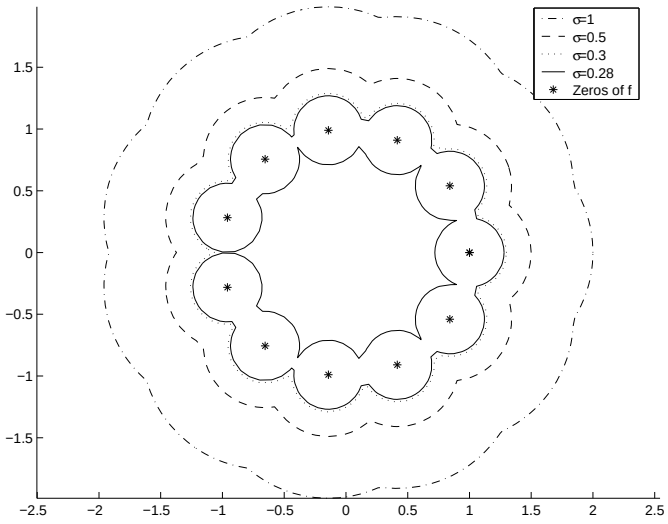

Figure 13: Level curves for $f(z) = \sigma_{\min}(A - zI)$ with $\tau = 0.1$

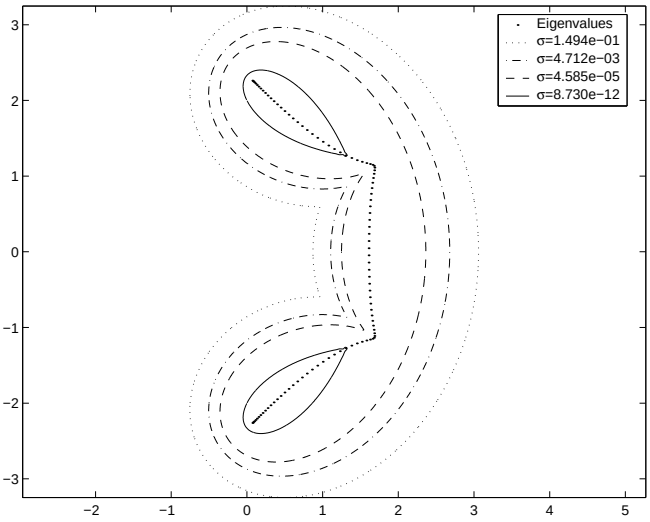

Figure 14: Level curves for $f(z) = \sigma_{\min}(A - zI)$ with $\tau = 0.01$

σ	Curve length	triangles	$\frac{l}{\tau}$	$\frac{10l}{\tau\sqrt{3}}$
$f(z) = z^{11} - 1$				
0.800	6.109	1812	611	3528
0.900	7.645	2356	765	4417
0.999	13.887	4454	1389	8020
1.000	24.477	5314	2448	14134
1.005	12.201	2694	1221	7050
1.050	9.484	2098	949	5480
1.200	7.988	1770	799	4614
$f(z) = \frac{z^5-1}{z}$				
1.200	7.996	180	80	462
1.650	12.781	282	128	740
2.000	11.090	243	111	641
3.000	10.504	227	106	612
1.200	8.017	1772	802	4631
1.650	12.899	2839	1290	7448
2.000	11.098	2451	1110	6467
3.000	10.509	2319	1051	6068
$f(z) = \sigma_{\min}(A - zI)$, A is normal				
0.280	16.434	356	165	953
0.300	9.308	200	94	543
0.500	9.669	216	97	561
1.000	12.552	280	126	728
0.280	18.492	4068	1850	10681
0.300	9.845	2164	985	5687
0.500	9.719	2144	972	5612
1.000	12.565	2768	1257	7258
$f(z) = \sigma_{\min}(A - zI)$, `GRCAR` problem				
8.730×10^{-12}	7.602	1675	761	4394
4.585×10^{-5}	16.858	3716	1686	9735
4.712×10^{-3}	17.813	3932	1782	10288
1.494×10^{-1}	19.168	4220	1917	11068

Table 2: Level curve length and the corresponding triangle count

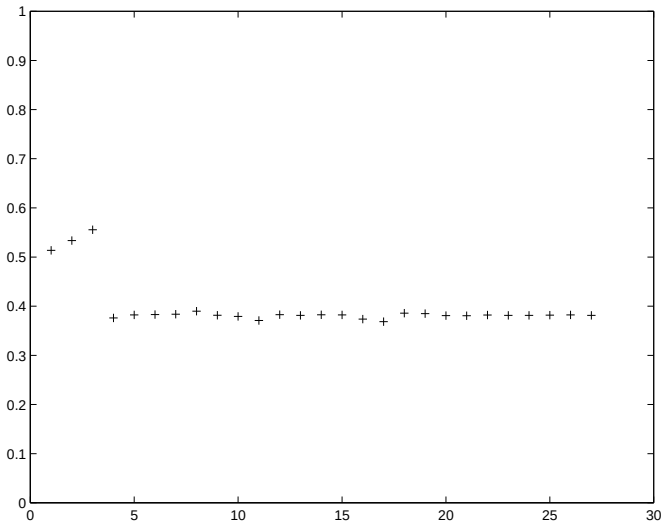

Figure 15: Ratio (Triangle Count)/$\frac{10l}{\tau\sqrt{3}}$.

of round-off errors. The proposed technique is able to handle singular points along the level curve without difficulty.

The fact that the computation of the $F-$orbit is separated from the bisection process means that one can parallelize the bisection on a cluster of machines [6]. This is important in the case of expensive functions like $\sigma_{\min}$ since the bisection processes on different triangles are completely independent and can be executed in parallel. This will speed up the path following algorithm by a large factor.

7 Acknowledgment

The authors are very grateful to J. Belward and J. Erhel for their helpful suggestions during the preparation of this paper.

References

[1] E.L. Allgower and K. Georg: Continuation and path following; *Acta Numerica*, 1-64 (1993).

[2] C.Bekas and E.Gallopoulos: COBRA: A hybrid method for computing the matrix pseudo spectrum. In *Copper Mountain Conference on Iterative Methods* (1998).

[3] G.H. Golub and C.F. Van Loan: *Matrix Computations*, 2nd Edition, The John Hopkins University Press, 1989.

[4] J. Huitfieldt and A. Ruhe: A new algorithm for numerical path following applied to an example from hydrodynamical flow', SIAM J. Sci. Statist. Comput. 11, 1181-1192 (1990).

[5] R. Mejia: CONKUB: A conversational path-follower for systems of nonlinear equations; J. Comput. Phys. 63, pp. 67-84, 1986.

[6] D. Mezher and B. Philippe: Parallel Pseudospectrum Calculations for Large Matrices; International Workshop Matrix Analysis and Applications, Neuchatel, August 2000.

[7] S.H. Lui: Computation of Pseudospectra by Continuation; *SIAM Journal on Scientific Computing*, Volume 18, Number 2, 565-573 (1997).

[8] B. Philippe and M. Sadkane: Computation of the Fundamental Singular Subspace of a Large Matrix. Linear algebra and its application 257, 77-104 (1997).

[9] W. Rudin: *Real and Complex analysis*, 3rd Edition, McGraw-Hill International Editions, 1986.

[10] Y. Saad: *Numerical methods for large eigenvalue problems*, Manchester University Press Series in Algorithms and Architectures for advanced scientific computing, 1992.

[11] H. Schwetlick, G. Timmermann, and R. Lösche: Path following for large nonlinear equations by implicit block elimination based on recursive projections. In J. Renegar, M. Shub, and S. Smale, editors, *The Mathematics of Numerical Analysis*. Proc. AMS-SIAM Summer Seminar Park City/Utah 1996, volume 32 of *Lectures in Applied Mathematics*, pp. 715-732. American Mathematical Society, Providence, RI (1996).

[12] H. Schwetlick and U. Schnabel: Iterative computation of the smallest singular value and the corresponding singular vectors of a matrix; Preprint IOKOMO-06-97, Techn. Univ. Dresden (1997).

[13] L.N. Trefethen: Pseudo spectra of matrices. In D.F. Griffith and G.A. Watson, editors, *14th Dundee Bennal Conference on Numerical Analysis* (1991).

[14] L.N. Trefethen: Pseudo spectra of Linear Operators. *SIAM Revue 3*, Volume 39, 383-406 (1997).

[15] C.W. Ueberhuber: *Numerical Computation, Methods, Software, Analysis*, Volumes 1,2. New York: Springer-Verlag 1997.

Unité de recherche INRIA Lorraine, Technopôle de Nancy-Brabois, Campus scientifique,
615 rue du Jardin Botanique, BP 101, 54600 VILLERS LÈS NANCY
Unité de recherche INRIA Rennes, Irisa, Campus universitaire de Beaulieu, 35042 RENNES Cedex
Unité de recherche INRIA Rhône-Alpes, 655, avenue de l'Europe, 38330 MONTBONNOT ST MARTIN
Unité de recherche INRIA Rocquencourt, Domaine de Voluceau, Rocquencourt, BP 105, 78153 LE CHESNAY Cedex
Unité de recherche INRIA Sophia-Antipolis, 2004 route des Lucioles, BP 93, 06902 SOPHIA-ANTIPOLIS Cedex

Éditeur
INRIA, Domaine de Voluceau, Rocquencourt, BP 105, 78153 LE CHESNAY Cedex (France)
http://www.inria.fr
ISSN 0249-6399